Laser and Particle Beams (2002), *20*, 585–588. Printed in the USA.

DOI: 10.1017/S0263034602204164

Nonlinear δf simulation studies of intense charged particle beams with large temperature anisotropy

EDWARD A. STARTSEV, RONALD C. DAVIDSON, AND HONG QIN
Plasma Physics Laboratory, Princeton University, Princeton, New Jersey 08543, USA

(RECEIVED 26 May 2002; ACCEPTED 18 June 2002)

Abstract

This article extends previous numerical studies of the stability properties of intense nonneutral charged particle beams with large temperature anisotropy ($T_{\perp b} \gg T_{\parallel b}$) to allow for nonaxisymmetric perturbations with $\partial/\partial\theta \neq 0$. The most unstable modes are identified, and their eigenfrequencies, radial mode structure, and nonlinear dynamics are determined.

Keywords: Anisotropy; Beam; Instability; Kinetic; Simulation

1. INTRODUCTION

It is well known that in neutral plasmas with strongly anisotropic distributions ($T_{\parallel b}/T_{\perp b} \ll 1$) a Harris-like collective instability may develop if there is sufficient coupling between the transverse and longitudinal degrees of freedom (Harris, 1959). Such anisotropies develop naturally in accelerators, where the longitudinal temperature of the accelerated beam of charged particles with charge q accelerated by a voltage V is reduced according to $T_{\parallel bf} = T_{\parallel bi}^2/2qV$ (for a nonrelativistic beam). In addition, the transverse temperature may increase due to nonlinearities in the applied and self-field forces, nonstationary beam profiles, and beam mismatch.

Previous studies of this anisotropy-driven instability in intense beams (Wang & Smith, 1982; Friedman *et al.*, 1990, 1992; Haber *et al.*, 1999; Startsev *et al.*, 2002) have shown that moderately intense beams with normalized beam intensity $s_b = \omega_{pb}^2/2\gamma_b^2\omega_f^2 \gtrsim 0.5$ are linearly unstable to short-wavelength, axisymmetric ($\partial/\partial\theta = 0$) perturbations with $k_z^2 r_b^2 \gtrsim 1$, provided the ratio of longitudinal to transverse temperatures is smaller than some threshold value. Here, $\omega_{pb}^2 = 4\pi\hat{n}_b e_b^2/\gamma_b m_b$ is the relativistic plasma frequency-squared, and $\omega_f = const.$ is the smooth-focusing frequency associated with the applied field. In this article, we extend our previous simulation studies of this instability (Startsev *et al.*, 2002) to the case with $\partial/\partial\theta \neq 0$.

In many practical applications, the transverse distribution function may be close to thermal equilibrium with temperature $T_{\perp b}$, and the longitudinal distribution can be described by a drifting Maxwellian distribution with temperature $T_{\parallel b} \ll T_{\perp b}$. This distribution is stable with respect to transverse perturbations (Davidson, 1998). For an arbitrary equilibrium distribution function, the stability problem cannot be solved analytically, and numerical simulation techniques must be employed. To investigate stability properties numerically, we use the nonlinear δf method (Parker & Lee, 1993) described below, as implemented in the Beam Equilibrium, Stability, and Transport (BEST) code (Qin *et al.*, 2000; Startsev *et al.*, 2002).

2. DESCRIPTION OF THE NONLINEAR δf SIMULATION CODE

In the smooth-focusing approximation, the transverse focusing force is modeled by $\mathbf{F}_{foc} = -\gamma_b m_b \omega_f^2 \mathbf{x}_\perp$, where $\omega_f = const.$, m_b is the particle rest mass, $\gamma_b = (1-\beta_b^2)^{-1/2}$ is the relativistic mass factor, $V_b = \beta_b c = const.$ is the axial velocity, and c is the speed of light. The solutions to the nonlinear Vlasov–Maxwell equations are expressed as $f_b = f_b^0 + \delta f_b$, $\phi = \phi^0 + \delta\phi$ and $A_z = A_z^0 + \delta A_z$, where (f_b^0, ϕ^0, A_z^0) are known equilibrium solutions ($\partial/\partial t = 0$). The perturbed potentials satisfy the equations (Qin *et al.*, 2000; Startsev *et al.*, 2002)

$$\nabla^2\delta\phi = -4\pi e_b \int d^3p\,\delta f_b, \tag{1}$$

$$\nabla^2\delta A_z = -\frac{4\pi}{c} e_b \int d^3p\, v_z \delta f_b, \tag{2}$$

Address correspondence and reprint requests to: Edward A. Startsev, Plasma Physics Laboratory, Princeton University, Princeton, NJ 08543, USA. E-mail: estarts@pppl.gov

where e_b is the particle charge, and $\delta f_b(\mathbf{x},\mathbf{p},t)$ is given by the weighted Klimontovich representation,

$$\delta f_b = \frac{N_b}{N_{sb}} \sum_{i=1}^{N_{sb}} w_{bi}\, \delta(\mathbf{x}-\mathbf{x}_{bi})\delta(\mathbf{p}-\mathbf{p}_{bi}). \tag{3}$$

Here, N_{sb} is total number of beam simulation particles, N_b is total number of actual beam particles, and the weight function is defined by $\omega_b \equiv \delta f_b/f_b$.

The nonlinear particle simulations are carried out by advancing the particle motion according to (Qin *et al.*, 2000; Startsev *et al.*, 2002)

$$\frac{d\mathbf{x}_{bi}}{dt} = (\gamma_b m_b)^{-1}\mathbf{p}_{bi}, \tag{4}$$

$$\frac{d\mathbf{p}_{bi}}{dt} = -\gamma_b m_b \omega_f^2 \mathbf{x}_{\perp bi} - e_b\left(\nabla\phi - \frac{v_{zbi}}{c}\nabla_\perp A_z\right), \tag{5}$$

$$\frac{dw_{bi}}{dt} = -(1-\omega_{bi})\frac{1}{f_{b0}}\frac{\partial f_{b0}}{\partial \mathbf{p}}\cdot\delta\left(\frac{d\mathbf{p}_{bi}}{dt}\right), \tag{6}$$

$$\delta\left(\frac{d\mathbf{p}_{bi}}{dt}\right) = -e_b\left(\nabla\delta\phi - \frac{v_{zbi}}{c}\nabla_\perp \delta A_z\right), \tag{7}$$

and updating the fields by solving the perturbed Maxwell's equations with appropriate boundary conditions at the cylindrical, perfectly conducting wall at radius r_w.

The δf approach is fully equivalent to the original nonlinear Vlasov–Maxwell equations, but the noise associated with representation of the background distribution f_b^0 in conventional particle-in-cell (PIC) simulations is removed. The typical gain in accuracy in δf simulations compared to PIC simulations with the same number of particles is $\epsilon_{\delta f}/\epsilon_{pic} = \overline{w}_{bi}$ (Parker & Lee, 1993; Qin *et al.*, 2000). This allows much more accurate simulations of the nonlinear dynamics and instability thresholds when $|\overline{w}_{bi}| \ll 1$. When the perturbation δf_b becomes comparable in magnitude with the background distribution function f_b^0, then the δf method becomes less accurate than a full PIC simulation. In the present article, a hybrid combination of the δf and PIC simulation methods is used (Startsev *et al.*, 2002), where the number density is calculated according to $\delta n_b = [1-\theta(\overline{w}_{bi})]\delta n_{\delta f} + \theta(\overline{w}_{bi})(n_{pic}-n_0)$, where $\theta(w)$ is a monotonic function of its argument such that $\theta(w\to 0)\to 0$ and $\theta(w\to 1)\to 1$. Here, $\delta n_{\delta f} = \int d^3p\,\delta f_b$ and $n_{pic} = \int d^3p f_b$.

In addition, the δf method can be used to study linear stability properties, provided all nonlinear terms in the dynamical equations (5)–(7) are neglected (Parker & Lee, 1993; Qin *et al.*, 2000). This corresponds to replacing the term $1-w_{bi}$ with 1 in Eq. (6) for the weights, and moving particles along the trajectories calculated in the unperturbed potentials (ϕ^0, A_z^0).

The δf method has been implemented in the three-dimensional PIC code (BEST) in cylindrical geometry with a perfectly conducting wall at radius r_w. Maxwell's Eqs. (1) and (2) are solved using fast Fourier transform techniques (FFT) in the longitudinal and azimuthal directions. The particle positions and weights are advanced using a second-order predictor–corrector algorithm. The code is parallelized using Message Passing Interface (MPI) with domain decomposition in the direction of beam propagation (Qin *et al.*, 2000; Startsev *et al.*, 2002).

3. SIMULATION RESULTS

In this section, we present the simulation results for a continuous, anisotropic beam in a constant focusing field. The self-consistent equilibrium distribution function ($\partial/\partial t = 0$) is taken to be

$$f_b^0 = \frac{\hat{n}_b}{(2\pi\gamma_b m_b)^{3/2}\gamma_b T_{\perp b} T_{\parallel b}^{1/2}} \exp\left\{-\frac{(p_z-\gamma_b m_b \beta_b c)^2}{2\gamma_b^3 m_b T_{\parallel b}}\right\} \times \exp\left\{-\frac{p_\perp^2/2\gamma_b m_b + \gamma_b m_b \omega_f^2 r^2/2 + e_b(\varphi_0 - \beta_b A_{z0})}{T_{\perp b}}\right\}, \tag{8}$$

where $\hat{n}_b$ is the beam density at $r=0$, and $T_{\perp b}$ and $T_{\parallel b}$ are the transverse and longitudinal temperatures. The equilibrium self-field potentials (φ_0, A_{z0}) are determined numerically from Maxwell's equations (Qin *et al.*, 2000). It is also assumed that the beam is located inside a grounded, perfectly conducting cylindrical wall at radius $r_w = 3r_b$, where $r_b = [\langle r^2\rangle]^{1/2}$ is the rms beam radius. Random initial perturba-

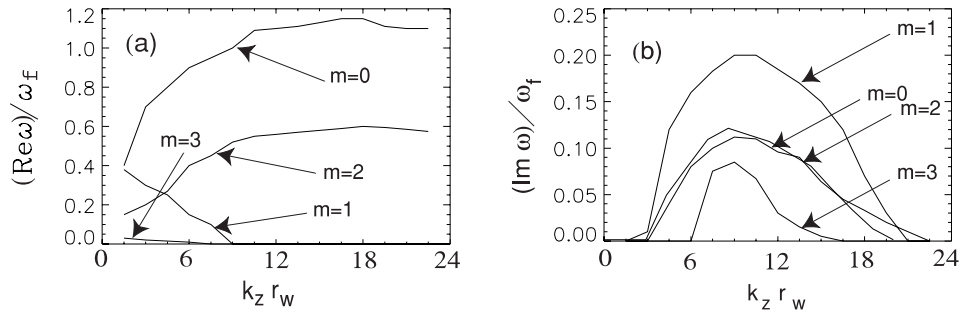

Fig. 1. Plots of normalized (a) real frequency $(Re\omega)/\omega_f$ and (b) growth rate $(Im\omega)/\omega_f$ versus $k_z r_w$ for $s_b = 0.95$.

https://doi.org/10.1017/S0263034602204164 Published online by Cambridge University Press

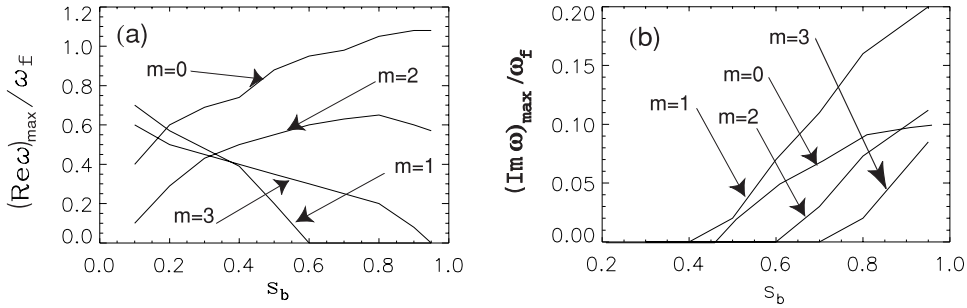

Fig. 2. Plots of normalized (a) real frequency $(Re\omega)_{max}/\omega_f$ and (b) growth rate $(Im\omega)_{max}/\omega_f$ at maximum growth versus normalized beam intensity s_b.

tions are introduced to the particle weights, and the beam is propagated from $t = 0$ to $t = 500\omega_f^{-1}$. The initial temperature ratio is taken to be $T_{\perp b}/T_{\parallel b} = 0.01$, and the simulations are performed in the beam frame with $\beta_b = 0$ and $\gamma_b = 1$. Typical numerical results are illustrated in Figures 1–5, where the simulations have been carried out over a wide range of normalized beam intensities $s_b = \omega_{pb}^2/2\gamma_b^2\omega_f^2$ ranging from $s_b = 0.1$ to $s_b = 0.95$.

Using the *linearized* version of the three-dimensional BEST code, Figures 1–3 show results of the δf simulations for perturbations with a spatial dependence proportional to $\exp(ik_z z + im\theta)$, where k_z is the axial wave number, and m is the azimuthal mode number. Figure 1 shows plots of the real and imaginary parts of the complex oscillation frequency ω versus normalized axial wave number $k_z r_w$, for $s_b = 0.95$ and azimuthal mode numbers $m = 0,1,2,3$. Note that the instability has a finite bandwidth with maximum growth rate at $k_z r_w \simeq 9$. The dependence of the maximum growth rate $(Im\omega)_{max}/\omega_f$ and the normalized real frequency $(Re\omega)_{max}/\omega_f$ at maximum growth on beam intensity s_b is shown in Figure 2. The maximum growth rate $(Im\omega)_{max}/\omega_f$ is an increasing function of beam intensity s_b. The dipole mode $m = 1$ has the largest growth rate. All modes are found to be stable in the region $s_b \leq 0.4$. The radial dependence of the eigenfunctions for the perturbed electrostatic potential using the linearized BEST code is illustrated in Figure 3 for $k_z r_w = 9$ and $s_b = 0.95$.

Figures 4 and 5 show typical simulation results using the *nonlinear* version of the three-dimensional BEST code for the case of normalized beam intensity $s_b = 0.8$. In Figure 4, the initial perturbation has a dominant initial excitation with $m = 1$ and $k_z r_w = 9$, and the time history of the perturbed density $\delta n_b = \int d^3p\,\delta f_b$ is plotted versus $\omega_f t$ at fixed axial position z and radius $r = 0.3r_b$. After the initial linear growth phase, note from Figure 4 that the instability saturates at a moderately large level with $|\delta n_{max}/\hat{n}_b| \simeq 0.1$.

Finally, shown in Figure 5 is a plot of the average longitudinal momentum distribution $F_b(p_z, t) = \int d^2p_\perp d^3x f_b$ versus p_z for a dominant initial excitation with $m = 1$ and $k_z r_w = 9$ (the case shown in Fig. 4). In Figure 5 the average distribution $F_b(p_z, t)$ at time $t = 200\omega_f^{-1}$ (thick curve) is compared with the initial distribution (thin curve). The formation of tails in axial momentum space in Figure 5 and the consequent saturation of the instability are attributed to quasi-linear stabilization.

4. CONCLUSIONS

The BEST code (Qin *et al.*, 2000), which implements the nonlinear δf scheme, has been used to investigate the stability properties of intense charged particle beams with large temperature anisotropy $(T_{\perp b}/T_{\parallel b} \ll 1)$ for perturbations with $\partial/\partial\theta \neq 0$. The simulation results clearly show that intense

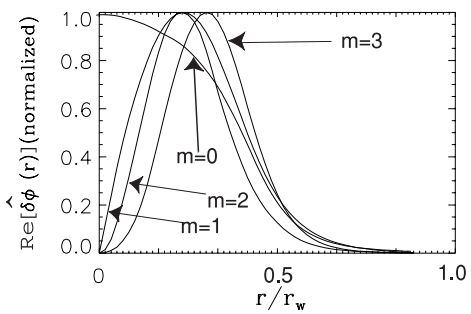

Fig. 3. Radial mode structure of the unstable $m = 0,1,2,3$ eigenfunctions for $k_z r_w = 9$ and $s_b = 0.95$.

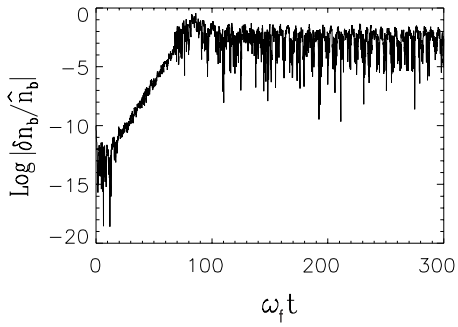

Fig. 4. Time history of normalized density perturbation $\delta n_{max}/\hat{n}_b$ for $s_b = 0.8$ at fixed z and $r = 0.3r_b$.

https://doi.org/10.1017/S0263034602204164 Published online by Cambridge University Press

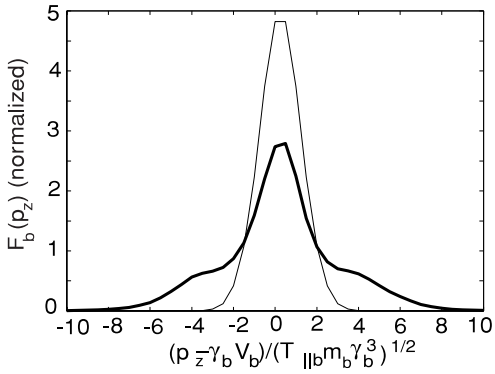

Fig. 5. Plot of average longitudinal momentum distribution $F_b(p_z)$ at time $t = 0$ (thin line) and $t = 200\omega_f^{-1}$ (thick line), for normalized beam intensity $s_b = 0.8$.

beams with $s_b \geq 0.4$ are linearly unstable to short-wavelength perturbations with $k_z r_w \geq 3$, provided the ratio of longitudinal and transverse temperatures is sufficiently small. In the nonlinear saturation stage, the total distribution function is still far from equipartitioned, and free energy is available to drive an instability of the hydrodynamic type.

REFERENCES

Davidson, R.C. (1998). Nonlinear stability theorem for high-intensity charged particle beams. *Phys. Rev. Lett.* **81**, 991–994.

Friedman, A., Callahan, D.A., Grote, D.P. & Langdon, A.B. (1992). Update on studies of equilibration processes in heavy ion beams. *Bull. Am. Phys. Soc.* **35**, 2121.

Friedman, A., Grote, D.P. & Haber, I. (1992). Three-dimensional particle simulation of heavy-ion fusion beams. *Phys. Fluids B* **4**, 2203–2210.

Haber, I., Friedman, A., Grote, D.P., Lund, S.M. & Kishek, R.A. (1999). Recent progress in the simulation of heavy ion beams. *Phys. Plasmas* **6**, 2254–2261.

Harris, E.G. (1959). Unstable plasma oscillations in magnetic field. *Phys. Rev. Lett.* **2**, 34–36.

Parker, S.E. & Lee, W.W. (1993). A fully nonlinear characteristic method for gyrokinetic simulation. *Phys. Fluids B* **5**, 77–86.

Qin, H., Davidson, R.C. & Lee, W.W. (2000).Three-dimensional multispecies nonlinear perturbative particle simulations of collective processes in intense particle beams. *Physical Review Special Topics on Accelerators and Beams* **3**, 084401–084409, 109901.

Startsev, E.A., Davidson, R.C. & Qin, H. (2002). Nonlinear δf simulation studies of intense charged particle beams with large temperature anisotropy. *Phys. Plasmas* **9**, 3138–3146.

Wang, T.F. & Smith, L. (1982). Transverse-longitudinal coupling in intense beams. *Part. Accel.* **12**, 247–260.

https://doi.org/10.1017/S0263034602204164 Published online by Cambridge University Press